PROGRESS IN PHOTOVOLTAICS: RESEARCH AND APPLICATIONS
Prog. Photovolt: Res. Appl. 2005; **13**:551–569
Published online 25 April 2005 in Wiley InterScience (www.interscience.wiley.com). DOI: 10.1002/pip.611

Research

Bulk and Surface Passivation of Silicon Solar Cells Accomplished by Silicon Nitride Deposited on Industrial Scale by Microwave PECVD

Wim Soppe*,†, Henk Rieffe and Arthur Weeber
Energy Research Centre of the Netherlands, ECN, P.O. Box 1, 1755 ZG Petten, The Netherlands

Bulk and surface passivation by silicon nitride has become an indispensable element in industrial production of multicrystalline silicon (mc-Si) solar cells. Microwave PECVD is a very effective method for high-throughput deposition of silicon nitride layers with the required properties for bulk and surface passivation. In this paper an analysis is presented of the relation between deposition parameters of microwave PECVD and material properties of silicon nitride. By tuning the process conditions (substrate temperature, gas flows, working pressure) we have been able to fabricate silicon nitride layers which fulfill almost ideally the four major requirements for mc-Si solar cells: (1) good anti-reflection coating (refractive index tunable between 2·0 and 2·3); (2) good surface passivation on p-type FZ wafers ($S_{eff} < 30$ cm/s); (3) good bulk passivation (improvement of IQE at 1000 nm by 30% after short thermal anneal); (4) long-term stability (no observable degradation after several years of exposure to sunlight). By implementing this silicon nitride deposition in an inline production process of mc-Si solar cells we have been able to produce cells with an efficiency of 16·5%.

Finally, we established that the continuous deposition process could be maintained for at least 20 h without interruption for maintenance. On this timescale we did not observe any significant changes in layer properties or cell properties. This shows the robustness of microwave PECVD for industrial production. Copyright © 2005 John Wiley & Sons, Ltd.

KEY WORDS: silicon nitride; microwave PECVD; surface passivation; bulk passivation; multicrystalline slicon; solar cells; internal quantum efficiency

* Correspondence to: Wim Soppe, Energy Research Centre of the Netherlands (ECN), PO Box 1, 1755 ZG Petten, The Netherlands.
†E-mail: soppe@ecn.nl

Contract/grant sponsors: Netherlands Agency of Energy and Environment; Netherlands Ministry of Economic Affairs; Netherlands Ministry of Education, Culture and Science; Netherlands Ministry of Public Housing, Physical Planning and Environment.

Received 25 August 2004
Revised 24 November 2004

1. INTRODUCTION

Amorphous silicon nitride (SiN_x:H) layers have become important components of multicrystalline (mc) silicon solar cells. The reason for this importance is a threefold functionality of the material for mc-Si solar cells.

The first function of silicon nitride is anti-reflection. By varying the ratio of Si/N in the SiN_x:H layer, the refractive index at 630 nm can be varied over a wide range between 1·9 and 2·5 which is ideal for both bare and glass-encapsulated cells.[1–3]

The second function of silicon nitride is surface passivation. The capabilities of SiN_x:H, grown by plasma enhanced chemical vapor deposition (PECVD) to reduce the recombination of charge carriers at the Si surface, have been known for more than 20 years.[4,5] In the meantime tremendous progress has been achieved, both in the quality of the surface passivation that can be obtained and in understanding the physical mechanisms behind the phenomenon of surface passivation.[6–16] Now that surface passivation using silicon nitride can be made as good as that using a thermal oxide, the material is increasingly used for the fabrication of high-efficiency silicon solar cells.[17–19] Big advantages of silicon nitride grown by PECVD with respect to thermal oxide are the low process temperature (typically in the range 300–400°C) and the short process time (typically a few minutes). The low process temperature is particularly important in the case of mc-Si wafers, where high-temperature processing, like thermal oxidation, may cause severe degradation of the bulk lifetime of charge carriers. Shorter process times are of immense importance for industrial manufacturing of solar cells.

The third function of silicon nitride is hydrogenation of the wafer if the layer undergoes a short thermal treatment after deposition. This hydrogenation induces passivation of defects and impurities in the bulk and can significantly increase the lifetime of minority charge carriers in the bulk of multicrystalline wafers.[20–27] The physical mechanisms of bulk passivation by hydrogenation are not yet completely understood. For instance, the hydrogen diffusion mechanism[28] and the role of an aluminum back surface field (Al-BSF) in this process[29–34] as well as the interaction between hydrogen and oxygen complexes in silicon[35,36] are still the subject of discussion. The benefits of bulk passivation by silicon nitride however are so evident that its implementation in the production process of mc-Si solar cells has become a priority for the PV industry.[37] The PECVD systems available for silicon nitride deposition, however, were until recently not designed for low-cost mass production of solar cells. The main reason for this is that these systems were developed for the semiconductor industry, where different demands with respect to throughput and layer quality apply than in the PV industry. In order to cater to specific demands from the PV industry, companies such as Roth&Rau,[38] Centrotherm,[39] MV-Systems,[40] OTB,[41] and others[42] have developed PECVD systems dedicated for mass production of solar cells. In this paper we will present a comprehensive overview of results that have been obtained with solar cell processing at ECN, using a pilot inline microwave PECVD system developed in collaboration between ECN and Roth&Rau.

The aim of this investigation is to establish the quality of deposited SiN_x:H layers in various regions of interest: optical properties, surface passivation, bulk passivation, production robustness.

2. THE MICROWAVE PECVD SYSTEM

2.1 System

Industrial systems for SiN_x:H deposition can be divided in two main groups: direct plasma systems with parallel plate reactors where the wafers are within the plasma zone and influence the plasma, and indirect plasma systems where the wafers are outside the plasma zone. The advantages for a indirect plasma system are the decoupling of the plasma and wafer transportation system which makes it possible to use wafers with arbitrary shape and size[16] and low ion energies, preventing surface damage and resulting in better surface passivation. Our pilot inline system developed in close cooperation with Roth&Rau is presented in Figure 1 and consists of an entry load-lock chamber, a deposition chamber with two linear microwave plasma sources and an exit load-lock chamber in which trays with an effective substrate area of $55 \times 55\,cm^2$ (which enables a batch size of, e.g., 25 wafers with size $10 \times 10\,cm^2$ or 9 wafers with size $15 \times 15\,cm^2$) are sequentially processed. For a single plasma module, the deposition time for one tray is in the range 3–6 min. The throughput of this system can easily be enlarged to industrial demands (1000–1500 wafers/h) by the addition of extra plasma modules.[43]

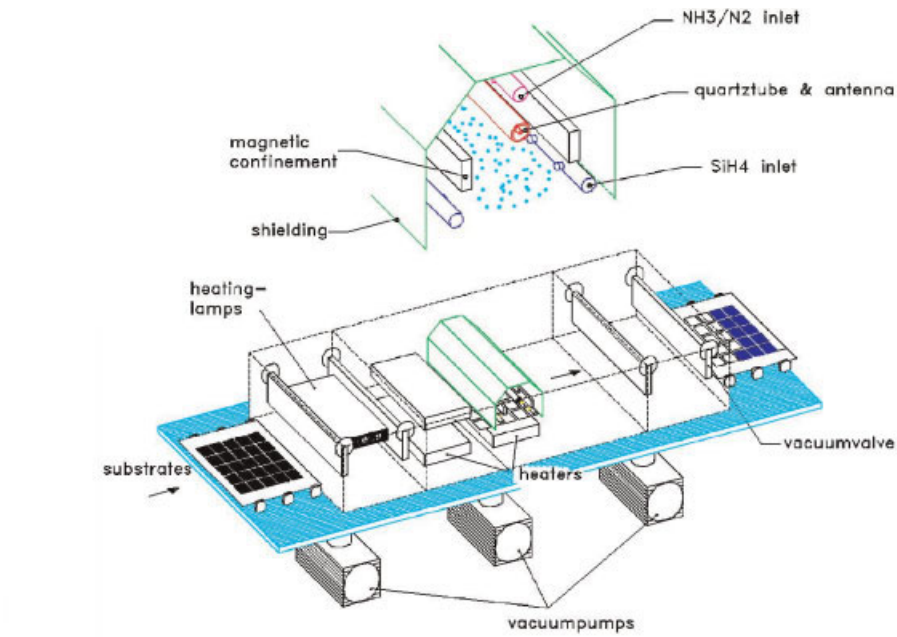

Figure 1. Side view of the pilot PECVD reactor. The insert shows a detailed view of the microwave source. The ECN system contains two quartz tubes, but for clarity only one quartz tube is shown. The photograph shows a production system, based on the same concept. The throughput of this production system is 1200 wafers/h (picture obtained from Roth&Rau)

In the entry chamber, the wafers are preheated by means of IR lamps. In the first part of the deposition chamber the wafers attain the deposition temperature (typically in the range 300–400°C). The deposition takes place in the central part of the deposition chamber, where the wafers underpass a linear plasma source.

The wafers cool down in the third part of the deposition chamber before entering the exit load lock chamber. Each vacuum chamber has an individual pumping system such that the evacuation of the chambers is not a major limiting factor for the throughput. The limiting factors for the throughput are the deposition time and the time needed for transport of the trays from one chamber to the next.

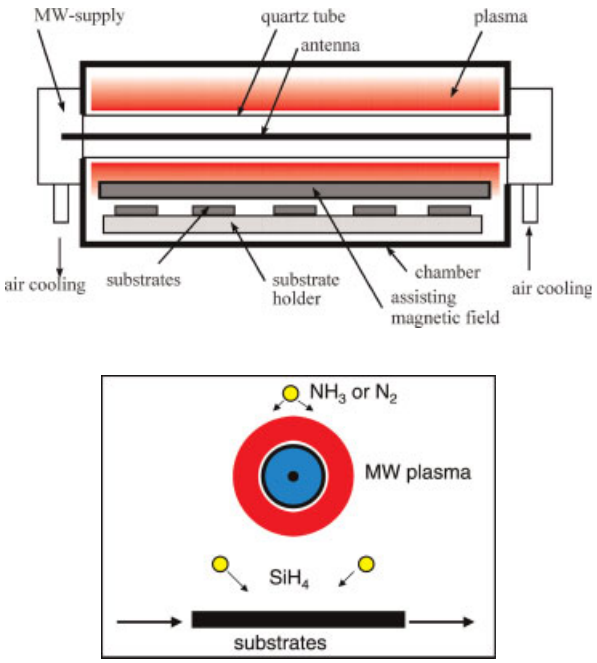

Figure 2. Cross-section of deposition chamber and microwave plasma source

2.2 *The linear microwave plasma source*

The plasma source in the reactor is a linear microwave (MW) plasma source, developed by Roth&Rau, consisting of two parallel quartz tubes with a Cu antenna inside. The source is operated at a microwave frequency of 2·45 GHz. The source also includes an arrangement of permanent magnets for electron confinement in the plasma (Figure 2). Different gasses can be used in the pressure range of about 0·01–1 mbar, depending on the plasma application. For deposition of silicon nitride, NH_3 or N_2 is fed in upstream, near the quartz tubes and SiH_4 is fed in downstream, near the substrate, both with typical flow rates in the range 100–200 sccm.

In comparison with conventional plasma sources this MW system has the following additional advantages:

- Due to the GHz frequency at which the source is operated, the plasma self bias is very low. Consequently, there is no ion bombardment of the substrate, which is a requirement to obtain excellent surface passivation.
- The utilization of the nitrogen containing source gases is more efficient. The depletion (i.e., the dissociation) of ammonia is more than 90%, and that of nitrogen is almost 50%. Higher depletion enables higher growth rates and better utilization of the process gases since the growth of silicon nitride depends on the concentrations of dissociated gas molecules. The depletion of ammonia and nitrogen in the MW plasma is typically one order of magnitude higher than for a conventional radiofrequency (RF) plasma. In order to obtain a stoichiometric silicon nitride by RF-PECVD the NH_3/SiH_4 flow ratio has to be about 10, whereas in our MW-PECVD system a flow ratio of about 1 suffices.[44]
- The linear source, in combination with accurately controlled substrate movement, reduces the problem of homogeneity of deposition to a one-dimensional problem, where for conventional, stationary RF-PECVD this is a more difficult two-dimensional problem.

The type of plasma in our MW system is a so-called surface wave sustained discharge,[45] and its physical properties differ significantly from those of more familiar plasma types such as inductive discharges and capacitive discharges.[46] In the MW plasma source wave launchers feed the waves simultaneously from both ends of the tube. The microwaves create a plasma with a certain spatial plasma density distribution. For low plasma powers (say 100 W) the plasma density extinguishes linearly in the axial direction so the plasma is confined to both ends of the tube. For higher microwave powers, the discharge extends along the full length of the tube and the superposition of the two linear decreasing plasma densities results in a constant axial plasma density

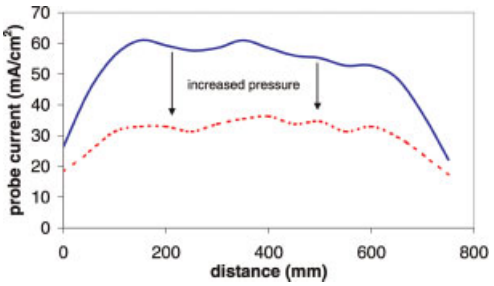

Figure 3. Ion current for NH_3 plasma, measured with Langmuir probes along the tube axis, for two different pressures. The probes are positioned about 15 cm from the quartz tube and have a bias voltage of −15 V. The dashed line presents the ion current at a higher pressure

along the entire tube. In the axial direction the plasma is confined due to shielding of the EM waves by the plasma.[47,48] This shielding occurs for plasma densities larger than the critical density n_c. For microwaves with the frequency of 2·45 GHz the critical density is $n_c = 7{\cdot}45 \times 10^{10}\,\mathrm{cm}^{-3}$ and this shielding condition is easily met for the MW powers applied in this source. The plasma thus acts as a coaxial waveguide for the microwaves.

Formation of standing waves is prevented by applying a pulsed mode for the microwave generation, in which different values for pulse duration t_{on} and pulse repetition time ($t_{on} + t_{off}$) for opposite wave launchers are used; t_{on} and t_{off} are typically in the range of 10 ms. In Figure 3 the ion current for a NH_3 plasma, measured with Langmuir probes along the tube axis is shown. The probes are positioned about 15 cm from the quartz tube and have a bias voltage of −15 V. The lateral distribution of the ion current density is a direct measure of the homogeneity of the plasma density along the tube axis, which has a length of 60 cm. It can be observed that for a zone width of at least 50 cm, the homogeneity of the plasma density is better than ±10%. A higher pressure results in a lower ion current because of a higher recombination of reactive species.

Deposition with the linear MW plasma source differs in two crucial aspects from remote plasma enhanced chemical vapor deposition (RPECVD), as applied by ISFH[14,49] using a Plasmalab 80 from Oxford Plasma Technology, albeit both systems work with microwaves. First, the plasma chemistry is different. The RPECVD is a true remote process in the sense that the only NH_3 is dissociated in the microwave plasma. SiH_4 is dissociated only by interactions with NH_x radicals. In the linear MW source, silane molecules can diffuse into the plasma zone and will be dissociated by NH_x radicals and by electrons. Second, the deposition geometry is different. For RPECVD deposition emanates from a point source, resulting in reduced uniformity in comparison with the linear MW source.

2.3 Growth rate and growth mechanisms

The growth rate of the SiN_x:H layers normally depends on process parameters such as gas flow, pressure, and temperature. We found that the growth rate of the SiN_x:H layer in our system primarily depends on the total flow of process gases, and depends only very little on process pressure or temperature. In principle, the growth rate also depends on the microwave power, but in a linear MW system the practical range of the MW power that can be applied is strongly restricted by homogeneity requirements. In Figure 4 the growth rate as a function of the total flow for a fixed ratio of process gases NH_3 and SiH_4 is displayed. It can be seen that the growth rate increases linearly with the total gas flow. This indicates that the growth rate—due to the high gas utilization—is limited by the supply of precursor gases. The applied MW power apparently is not a limiting factor in the production of reactive species in the flow range investigated.

Little is known yet about the details of the chemical reactions in the plasma in the microwave PECVD system. A model for NH_3/SiH_4 plasmas has been proposed by Smith,[50] and Hanyaloglu and Aydil[51] and Kessels *et al.*[52] have proposed two similar models for N_2/SiH_4 plasmas.

For NH_3/SiH_4 plasmas the gases will be dissociated in NH_x and SiH_x species. It has been speculated by Smith that these species combine in the plasma into tetraaminosilane $Si(NH_2)_4$ which acts as the main precursor for layer growth. In this model the formation of $Si(NH_2)_4$ is the rate-limiting step. This model therefore predicts an increase of the growth rate with increasing pressure, which is not in correspondence with our observations.

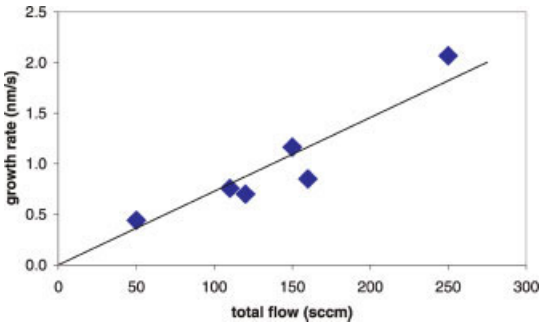

Figure 4. Growth rates of SiN_x:H as a function of total flow using NH_3 and SiH_4 with a flow ratio of 1·0

Hanyalogly and Aydil suggested that in N_2/SiH_4 plasmas, silicon nitride layer growth proceeds through attachment of SiH_3 species to the surface followed by nitridation of the top of the film by vibrationally excited N_2 species. Kessels *et al*. conclude that the surface layer is nitrided by N radicals rather then by excited N_2. According to these growth models, the deposition rate depends on the flux of species arriving at the substrate. Since the densities of N and SiH_3 species depend on the production rate of these species and therefore on the flow of the precursor gases, we conclude that the models of Hanyaloglu and Kessels can be reconciled with our observations for microwave PECVD.

In the next sections we will evaluate the models mentioned with respect to other observations.

3. OPTICAL PROPERTIES OF SiN LAYERS

In order to function as an anti-reflection coating on crystalline Si solar cells, the silicon nitride layers should have a refractive index of either about 2·0 or 2·3, for respectively bare cells and encapsulated cells.[1] In addition, the absorption of light in the layers should be as small as possible for wavelengths where the solar cell is active (300–1150 nm). This means that the optical bandgap of the SiN_x:H should be larger than about 4 eV. Concisely: the total transmittance $T(\lambda) = 1 - R(\lambda) - A(\lambda)$ should be as large as possible for wavelengths between 300 and 1150 nm.

For stoichiometric silicon nitride with a refractive index of about 1·9, the optical bandgap[53] is 5·3 eV. The optical gap decreases with increasing silicon contents until finally an optical gap of 1·8 eV for hydrogenated amorphous silicon is obtained.[54] The decrease of the optical gap is due to an increase of the Si–Si coordination number and this increase produces narrowing of the Si–Si σ and σ^* bands.[53]

Optical properties of SiN_x:H layers grown on Cz-wafers were measured with spectroscopic ellipsometry (SE) and with a Filmetrics reflectometer. Refractive index and absorption of the SiN_x:H layers can be tuned by the flow ratios NH_3/SiH_4 or N_2/SiH_4 and by the pressure. Smaller flow ratios lead to the growth of more Si-rich films with higher refractive indices and with higher absorption coefficients. This trend can be observed in Figures 5 and 6.

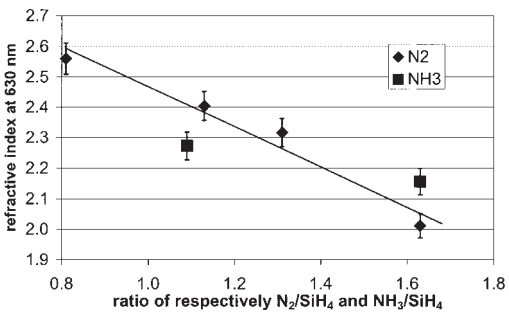

Figure 5. Refractive index as a function of N_2/SiH_4 and NH_3/SiH_4 flow ratio. Values displayed are the indices at 630 nm

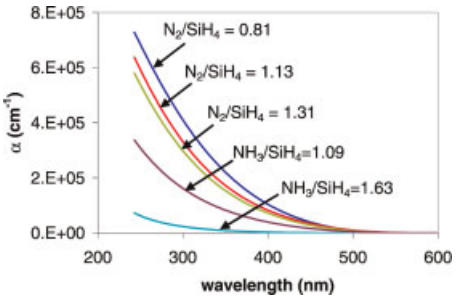

Figure 6. Absorption coefficient of SiN_x:H for various N_2/SiH_4 and NH_3/SiH_4 ratios

Figure 5 shows that irrespective of whether N_2 or NH_3 is used as process gas, approximately the same gas flow ratios of N_2/SiH_4 or NH_3/SiH_4 are required to obtain a given refractive index at 630 nm. This surprising result is explained by residual gas analysis (RGA) of the plasma. RGA shows that the depletion of N_2 in the MW plasma is about half of that for NH_3. This implies that for a given molar flow of either N_2 or NH_3, the concentration of NH_x species in the plasma is the same.[55] Probably, the N/Si ratio in the deposited layer will also be the same for layers grown with the same gas flow ratio N_2/SiH_4 or NH_3/SiH_4.

For equivalent refractive indices at 630 nm, SiN_x:H layers deposited with N_2 have higher absorption at shorter wavelengths than layers deposited using NH_3. This effect is demonstrated in Figure 6 and implies that the absorption $k_{<500\,\mathrm{nm}}$ is not uniquely linked to the refractive index $n_{630\,\mathrm{nm}}$. Apparently, the dispersion $\mathrm{d}n/\mathrm{d}\lambda$ is different for layers grown with N_2 than for layers grown with NH_3.

Pressure, total flow and substrate temperature are other important factors for the optical properties of the SiN_x:H films. We observe (Figures 7 and 8) that for a given flow ratio the refractive index increases with increasing pressure, and increases slightly with increasing total flow or substrate temperature. The increased refractive index with increased pressure can be explained with an adaptation of the models by Hanyaloglu and Kessels. In our model we assume the following dissociation chains for NH_3, N_2 and SiH_4:

The main dissociation chain of NH_3, which is fed in near the quartz tube is:

$$NH_3 + e \rightarrow NH_2 + H + e \tag{1}$$

For SiH_4, which is fed in just above the samples, and more remote from the quartz tube, the following dissociation reactions can be expected:

$$SiH_4 + e \rightarrow SiH_3 + H + e \tag{2}$$

$$SiH_4 + e \rightarrow SiH_2 + 2H + e \tag{3}$$

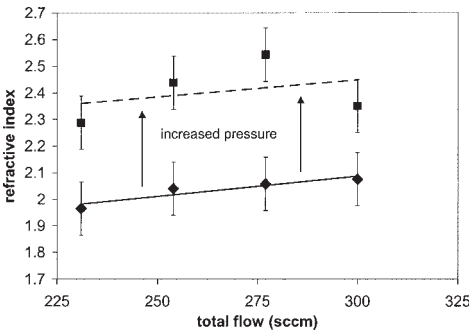

Figure 7. Refractive index as a function of total flow ($SiH_4 + NH_3$) for two different process pressures. The dashed line shows the effect at higher pressure

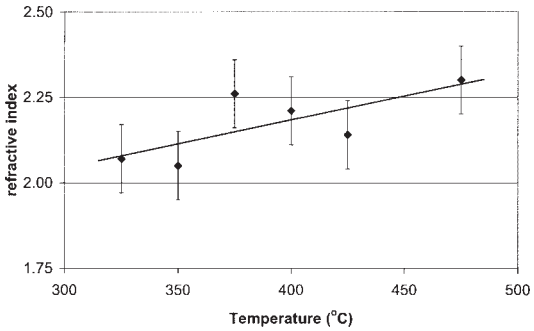

Figure 8. Refractive index as a function of the substrate temperature

$$SiH_4 + NH_2^* \rightarrow SiH_3 + NH_3\uparrow \tag{4}$$

$$SiH_4 + H \rightarrow SiH_3 + H_2\uparrow \tag{5}$$

The $\uparrow$ sign indicates formation of a gas molecule that will very probably escape from the plasma zone, and will not contribute to the deposition process anymore. For higher pressures the plasma is more closely confined near the quartz tube and the electron density at more remote distances is lower than for lower pressures. Therefore, reactions (2) and (3) will be suppressed at higher pressures, and reactions (4) and (5) will obtain a larger share. In particular the larger share of ammonia removing reaction (4) will lead to formation of more silicon-rich layers, and therefore to layers with a higher refractive index. For the case of N_2 as process gas, instead of NH_3, a similar model can be applied, where reaction (5) can be omitted and reaction (1) is replaced by:

$$N_2 + e \rightarrow 2N + e \tag{6}$$

and reaction (4) is replaced by:

$$SiH_4 + N \rightarrow SiH_2 + NH_2 \tag{7}$$

plus

$$SiH_4 + NH_2 \rightarrow SiH_3 + NH_3\uparrow \tag{8}$$

leading to the same conclusions as for the case of NH_3.

The increase of the refractive index in the cases mentioned above is generally accompanied by an increase of the absorption k. This enhanced absorption is probably due to an increased Si–Si coordination in the films. In the next sections we will see that high refractive indices often correlate with good passivation by the SiN_x:H layers. So in practice we often have to find a balance between good passivation and good optical transmittance of the layers.

Such a trade-off has also to be made in the choice of the refractive index of SiN_x:H layers for cells which will be encapsulated. As stated before, the ideal refractive index of anti-reflection coatings for encapsulated cells is about 2·3. However, given the appreciable absorption of blue light for silicon nitride layers with refractive indices of 2·3 we found that the total transmittance of silicon nitride commonly is best for $n = 2{\cdot}1$–$2{\cdot}2$.

4. SURFACE PASSIVATION

In order to establish the quality of surface passivation by SiN_x:H we processed p-type FZ wafers from Wacker. The wafers are polished on one side and shiny etched on the other side and have a resistivity of about 1·5 Ω cm

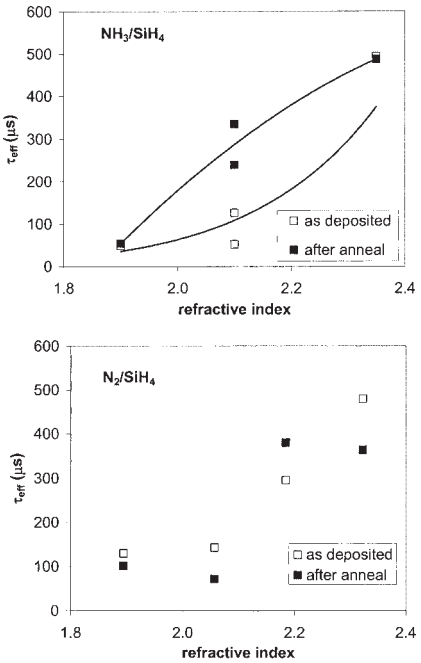

Figure 9. Effective lifetime of minority charge carriers τ_{eff} in FZ wafers, coated on both sides with SiN_x:H layers before and after a thermal anneal. The SiN_x:H layers have been grown using $NH_3 + SiH_4$ and $N_2 + SiH_4$ as process gases. Values are averages over four samples, spanning the entire width of the reactor during deposition

and thickness of 325 μm. Prior to both-side deposition of SiN_x:H, the wafers obtained an RCA clean. The surface recombination velocity was determined using the quasi-steady-state photoconductance (QSSPC)[56] method. Thermal stability of the films was determined by repeating the QSSPC measurements after a thermal anneal of the wafers. The thermal anneal was identical to the one used for co-firing of front and rear side metallization of mc-Si solar cells (see next section).

We investigated the dependence of the surface passivation on process parameters: pressure, substrate temperature, NH_3/SiH_4 or N_2/SiH_4 ratio and total gas flow Φ. The general trend is that a certain minimum pressure p_{min} is required to achieve surface passivation. Optimum surface passivation is obtained for deposition temperatures between 350 and 400°C and flow ratios leading to a refractive index of 2·3–2·4 (Figure 9). These refractive indices are obtained for NH_3/SiH_4 and N_2/SiH_4 ratios of respectively, about 1·1 and 1·3.

For these deposition conditions we obtain values for the effective lifetime of minority charge carriers τ_{eff} larger than 500 μs, at injection levels of $1{\cdot}5 \times 10^{15}\,\text{cm}^{-3}$. Assuming a realistic upper limit of the bulk lifetime in this material of 1 ms, this implies a surface recombination velocity S_{eff} of less than 30 cm/s. This is a quite good result, taking into account that the processing did not take place under clean room conditions. Moschner *et al.*[57] obtained with a similar inline microwave PECVD system, but in a clean-room environment, values of τ_{eff} of about 700 μs on *p*-type FZ wafers for SiN_x:H coatings with a refractive index of about 2·3.

For the N_2 depositions, we found good values of τ_{eff} in the range 300–400 μs, for a refractive index above 2·1, which corresponds to an N_2/SiH_4 ratio of 1·3–1·6. As such this is the first reported high-quality surface passivation of SiN_x:H obtained with only N_2 and SiH_4 as precursor gases. Schmidt *et al.*[12] have reported good surface passivation (S_{eff} of less than 10 cm/s) for refractive index above 1·9 using an NH_3/SiH_4:N_2 gas mixture.

An interesting feature of silicon nitride layers deposited with NH_3/SiH_4 and a refractive index of about 2·1 is that the surface passivation is further improved after thermal annealing. Layers with a refractive index of about 2·3 appear to be very stable under thermal annealing. This seems to be in contrast with findings of Lenkeit *et al.*[13,14] who found severe degradation for this type of silicon nitride, deposited with RPECVD.

The improvement of the surface passivation for layers grown with NH_3/SiH_4 with a refractive index of about 2·1, after thermal anneal, on the other hand, is completely in line with findings of these authors. For layers deposited with N_2/SiH_4 the surface passivation is hardly affected by a thermal anneal.

5. CELL PROCESSING

We optimized the PECVD process conditions for SiN_x:H deposition on mc-Si solar cells by varying the process parameters and comparing the *I–V* characteristics and internal quantum efficiencies (IQE) of the processed cells with those of ingot-neighbor cells which underwent a reference scenario. In the reference scenario, the deposition of the SiN_x:H is the last step of the processing. Consequently, the SiN_x:H layers are not annealed, and hydrogenation of the silicon wafer from the layer will not take place. Assuming that optical properties of the layers are the same as for the experimental scenario, comparison of cells processed according to the reference scenario with cells processed according to the experimental scenario should provide evidence of bulk passivation by annealing of SiN_x:H. Details of the cell processing scenarios can be found in Table I. All steps are inline processes. In order to avoid blistering of the silicon nitride layer during the contact-firing step, it is important to remove the phosphorus glass layer thoroughly. This blistering is caused by hydrogen diffusing from the film, forming gas bubbles at the wafer interface if there is a barrier preventing diffusion into the wafer. This phenomenon is not unique for silicon nitride, but has been observed for amorphous silicon films as well.[58] At ECN we have developed a dedicated wet chemical clean for this purpose, but Hauser *et al*.[59] have shown that—in an RF-PECVD system—a short ammonia plasma etching step prior to the SiN_x:H deposition also suffices to avoid this problem.

The PECVD process parameters that were varied were gas flow ratio (NH_3/SiH_4 and N_2/SiH_4), pressure, wafer temperature, and total gas flow. In each experiment we processed cells from neighboring mc-Si wafers and we used a statistical analysis tool Statgraphics[60] to determine the statistical significance of the results. With this tool a least-squares fit to a second-order model was made including the effect of using different neighboring wafer types:

$$y_n = \beta_0 + \sum_{i=1}^{k} \beta_i x_i + \sum_{i=1}^{k} \beta_{ii} x_i^2 + \sum_{i}^{i<j} \sum_{j} \beta_{ij} x_i x_j + w_n + \varepsilon \tag{9}$$

with y_n the fitted parameter (V_{oc} or J_{sc}) as a function of process parameters and neighboring wafer type, β coefficients, x the process variables (gas flow ratio, pressure), w_n is the effect of the n^{th} neighboring wafer type,[61] and ε the random error term. The quality of the fit can be investigated by comparing the fitted parameter to the observed one.

The experiments with NH_3/SiH_4 were divided into three series. The first series was to determine the effects of flow ratio and pressure and contained nine different runs. The second series was performed to determine the effects of deposition temperature and pressure and comprised eight runs. The third series was performed to establish the effect of total flow and contained five runs. In each experiment we coated four wafers of

Table I. Process schemes of mc-Si solar cells

Firing-through	Reference
Alkaline saw damage etch or acid texturing etch	Alkaline saw damage etch or acid texturing etch
Emitter formation (50 Ω/sq)	Emitter formation (50 Ω/sq)
P-glass removal	P-glass removal
PECVD SiN_x:H	Screenprinted front-side metallization
Screenprinted frontside metallization	Screenprinted Al rear-side metallization
Screenprinted Al rear-side metallization	Co-firing of front- and rear-side metallization
Co-firing of front- and rear-side metallization	PECVD SiN_x:H

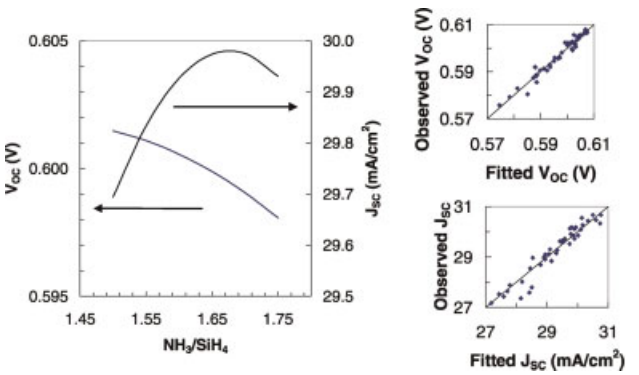

Figure 10. Main effect of the NH_3/SiH_4 flow ratio on J_{sc} and V_{oc} of mc-Si cells, fabricated with firing-through SiN_x:H layers. Statistics show that the effect on J_{sc} is real with a certainty of 90% (More precisely: the effect is different from zero at the 90% confidence limit). For V_{oc} the certainty is more than 95%. The inserts show the observed versus the fitted values for V_{oc} and J_{sc}

$12{\cdot}5 \times 12{\cdot}5\,cm^2$ or five wafers of $10 \times 10\,cm^2$. We used neighbor wafers to ensure equal run-to-run wafer material quality in each experiment.

The depositions with N_2/SiH_4 comprised one experiment of 16 runs in which we applied $12{\cdot}5 \times 12{\cdot}5\,cm^2$ wafers, and coated 4 wafers per deposition. An acid etch was applied for saw damage removal and texturing. We used 4 sets of 16 neighbors to determine the effects of process pressure, flow ratio and total flow on the solar cell performances.

5.1 Effects of flow ratio

Changing the ratio of NH_3/SiH_4 or N_2/SiH_4 is the most straightforward way to vary the N/Si ratio in the film. The N/Si ratio in the film determines the refractive index and strongly effects the surface passivation of the SiN_x:H layers. The so-called main effect of the flow ratio on the electrical performances of mc-Si cells is smaller, but still significant, as illustrated in Figure 10 for NH_3/SiH_4 depositions and in Figure 11 for N_2/SiH_4 depositions. The inserts show plots of the observed V_{oc} and J_{sc} against the fitted values. The observed values scatter randomly around the *observed = fitted* line, justifying the model used.

Highest V_{oc} is obtained for silicon rich layers (obtained with small NH_3/SiH_4 or N_2/SiH_4 ratios) and this is at least partly due to optimum surface passivation for Si-rich layers. The current, however, depends strongly on the optical properties of the layers. The ideal refractive index of AR coatings on cells (in air) is about 2·1–2·2, and this value is obtained for higher NH_3/SiH_4 or N_2/SiH_4 ratios of about 1·6.

For highest cell efficiencies a compromise is required between conditions for high V_{oc} and high J_{sc}. For depositions with NH_3 and SiH_4 this leads to maximum $V_{oc} \times J_{sc}$ for $NH_3/SiH_4 \simeq 1{\cdot}6$. For depositions with N_2 and SiH_4 we find maximum $V_{oc} \times J_{sc}$ for $N_2/SiH_4 \simeq 1{\cdot}5$.

5.2 Effect of pressure

The process pressure affects the chemistry in the plasma by affecting the radius of the plasma zone and by affecting the residence time of process gases. As a result the composition of the SiN_x:H layers and their passivating properties vary with varying process pressures.

For cell processing with SiN_x:H layers grown with NH_3 and SiH_4, an optimum deposition pressure was established. For lower pressures the bulk passivation is reduced which affects both V_{oc} and J_{sc}. For higher pressures V_{oc} saturates but J_{sc} decreases due to absorption as a result of the higher refractive index. These effects can be seen in Figure 12. Note that the IQEs are corrected for reflection of the silicon nitride layers, but not for the absorption of these layers.

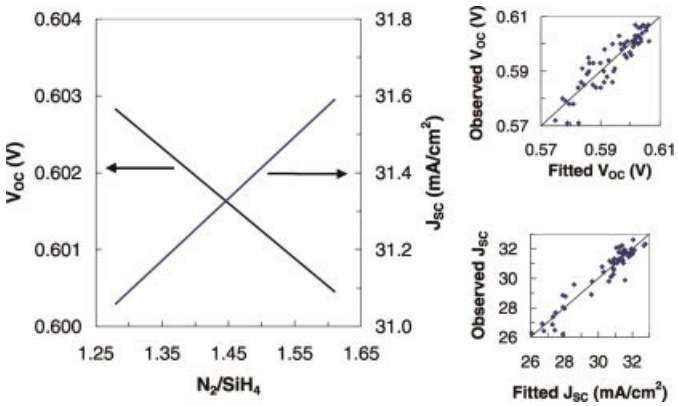

Figure 11. Main effect of the N_2/SiH_4 flow ration on J_{sc} and V_{oc} of mc-Si cells, fabricated with firing-through SiN_x:H layers. Statistics show that the effect on J_{sc} is real with a certainty of more than 95%. For V_{oc} it is 85%. The inserts show the observed versus the predicted values for V_{oc} and J_{sc}

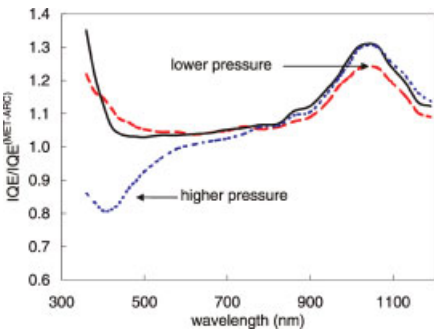

Figure 12. Relative internal quantum efficiencies of cells made with silicon nitride, grown with NH_3 and SiH_4, deposited at various pressures. IQEs are relative to that of a cell that underwent the reference scenario. The lower pressure shows a decreased red response and the higher pressure a decreased blue response

5.3 Effect of substrate temperature

We varied the substrate temperature between 325 and 400°C, and within this range the temperature did not affect the cell performances. From previous experiments[25] we know that the hydrogen content decreases and the surface passivation improves in general with increasing substrate temperature in the range 200–400°C, but in the range 325–400°C the changes are not significant.

Figure 13 illustrates these findings. The figure shows the IQEs of cells with SiN_x:H coatings deposited at various temperatures, relative to the IQE of a reference neighboring cell made (see Table I). The large increase of IQE between 800 and 1200 nm is due to bulk passivation. The gain of IQE for the cell which obtained the SiN_x:H coating at 400°C is slightly smaller than for the lower substrate temperatures. This can be attributed to slightly smaller hydrogen contents in the layers deposited at 400°C.

The increase of IQE at smaller wavelengths between 350 and 450 nm suggests that the firing-through SiN_x:H process also leads to better passivation in the front surface region. The total gain of IQE leads to an increase of V_{oc} from 589 mV for the reference cells to 612 mV for the cells from the firing-through scenario.

5.4 Effects of total flow

The electrical performances of mc-Si solar cells are quite sensitive to the total flow during the silicon nitride deposition in the case of NH_3 and SiH_4 as process gasses. We varied the total flow from 185 to 355 sccm,

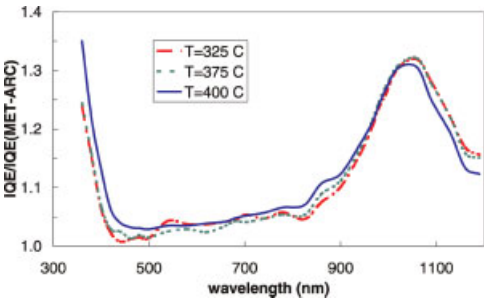

Figure 13. Relative internal quantum efficiencies of cells made with silicon nitride deposited at various substrate temperatures. NH_3 and SiH_4 were used as process gases. IQEs are relative to that of a cell that underwent the reference scenario

keeping the ratio NH_3/SiH_4 constant at 1·6. V_{oc} increases with increasing total flows and J_{sc} has an optimum for about 280 sccm. Best cell performances are found for a total flow of 280 sccm.

The effect of the flow rates for depositions with N_2 and SiH_4 was investigated in a narrower range: between 200 and 250 sccm. Within this range, the total flow does not have a significant effect on V_{oc} or J_{sc}.

5.5 *Overall effects*

The optimum SiN_x:H for the front side of mc-Si solar cells is the result of a delicate trade-off of various properties: total transmittance, surface passivation and bulk passivation. High transmittance requires a refractive index of 1·9–2·1, which is obtained for N_2/SiH_4 and NH_3/SiH_4 ratios in the range 1·4–1·6. Best surface passivation of FZ wafers is obtained for small flow ratios of 1·1, which results in a refractive index of about 2·3. These layers are highly absorbing.

Our experiments provide clear evidence for the capability of SiN_x:H to improve the effective lifetime of minority charge carriers in the bulk of mc-Si wafers (bulk passivation) if the layer is annealed as in the firing process of screenprinted metallization.

The most favorable SiN_x:H layer thus is a compromise, but nevertheless it is a very effective layer. In comparison with the non-passivating alternative: the formerly commonly used TiO_2 layer, application of SiN_x:H typically leads to a gain of 20 mV and an increase of 10–15% of the total cell performance.

Results of *I–V* measurements of the cells obtained for optimum deposition conditions are displayed in Table II. The results underline the importance of front surface passivation in order to obtain high-efficiency cells. By using different wafer material and more advanced processing, but using the same recipe for SiN_x:H deposition we were able to increase cell efficiencies from 14·7 to 16·5%. This improvement resulted merely because the lower-doped emitter allowed better surface passivation, and therefore a significantly better internal quantum efficiency at short wavelengths.

Table II. *I–V* characteristics of mc-Si cells with SiN_x:H deposition, obtained for optimum deposition conditions

Process gas		Emitter sheet resistance (Ω/sq)	J_{sc} (mA/cm^2)	V_{oc} (mV)	$J_{sc} \times V_{oc}$ (mA/cm^2 V)	Efficiency (%)
NH_3	N_2					
×		50	32·1	605	19·4	14·7
	×	50	32·3	600	19·4	14·7
×		65	34·5	623	21·5	16·5

Values in the first two rows are means over four cells (12·5 × 12·5 cm), covering the entire width of the deposition tray. The last row shows the results of the best cell, measured at NREL, using a more advanced inline processing and Si wafers from another batch, but with the same SiN_x:H deposition process as for the first row.

6. STABILITY OF PECVD PROCESS

We have performed an endurance test to check the stability of the microwave PECVD process over a long period of use. Important topics we wanted to investigate were:

1. What is the total deposition time that a system can run continuously without flake formation? The MW-PECVD system has a downstream configuration: the tray with wafers moves underneath the quartz tubes. Because of that, silicon nitride flakes formed by parasitic deposition can fall on the wafers. Large flakes or large numbers of small flakes will result in visually unacceptable cells. Moreover, solar cell efficiency losses will occur due to reflection losses. A drastic solution is to apply an upstream configuration, but this results in small uncoated areas on all wafers due to shadowing by suspension clamps.
2. Do the passivation properties change with increasing deposition time? These properties could change because of small changes in the plasma due to parasitic depositions.

We used an industrial process scheme for making solar cells as discussed in Section 5. Multicrystalline $12{\cdot}5 \times 12{\cdot}5$ cm wafers were used as starting material. The wafers were distributed over 19 batches. We used neighboring wafers to exclude differences in material quality. After different times of plasma processing a batch of wafers was deposited using the standard ECN process with NH_3 and SiH_4 as process gasses. Together with the multicrystalline wafers a piece of polished monocrystalline material was deposited for optical characterization of the SiN_x:H layer. After about 8 h plasma processing the system was cooled down to room temperature during the night. After heating up on the next day the processing was resumed. After about 17 h there was another break during night. The total time with plasma on was 20 h.

6.1 Number of flakes and optical properties

During the first period of about 8 h plasma time hardly any flakes fall from the quartz tubes or from the walls of the system on the wafers. During the nights the system was cooled down. The first deposition the next day showed a larger number of small flakes on the wafers. However, the number of flakes reduced tremendously after a second deposition. The same was observed for the next day.

In an industrial environment the system will probably not be cooled down during normal operation and this effect will be of little importance.

The refractive index n measured at 630 nm was 2·10 and constant over 20 h plasma time. The extinction coefficient k did not change either. However, the layer thickness increased a few nanometer, but the increase is less than 5%. This can be seen in Figure 14.

6.2 Solar cell results

Figure 15 shows the average V_{oc} and J_{sc} of the different batches over a plasma time of 20 h. It can be seen that V_{oc} does not change over that time. J_{sc} increases from about 28·4 to 29·1 mA/cm^2. This increase of about 3% cannot be explained by the small change in layer thickness of the ARC.

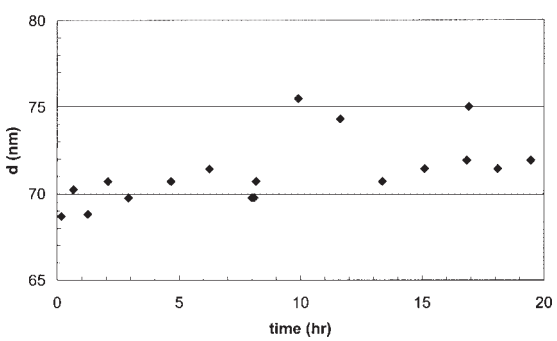

Figure 14. Thickness of the deposited SiN_x:H layers over 20 h plasma time

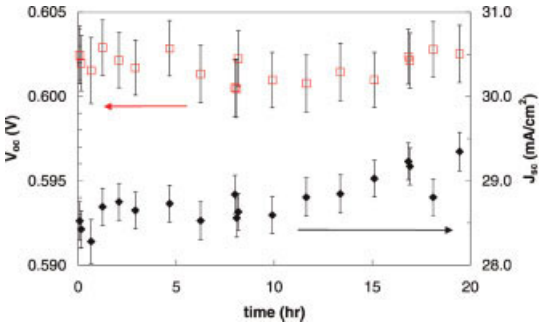

Figure 15. Average V_{oc} and J_{sc} over 20 h plasma time. The bars indicate the 95% confidence intervals. No overlap between the confidence intervals means that values differ with a certainty of more than 95%

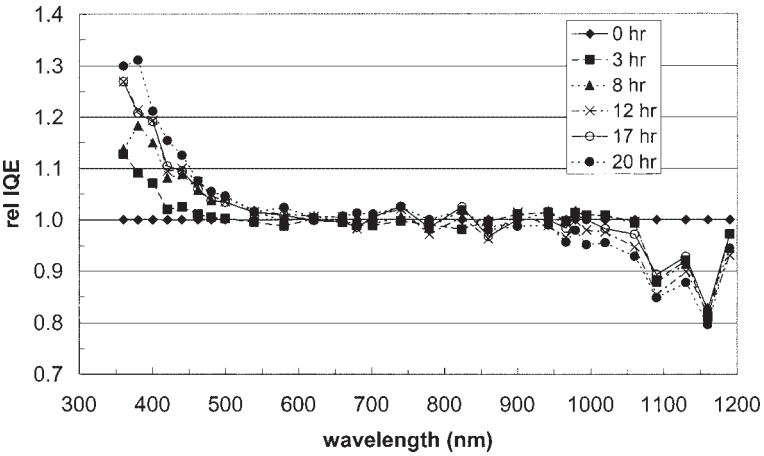

Figure 16. Relative IQE measurement of one type of neighbouring cell at different plasma times

Since fill factor is constant over all the batches the efficiency η will increase proportionally to J_{sc}. To find out the reason for this increase, IQE measurements were performed on one set of neighboring wafers. The IQE after different plasma times is presented in Figure 16. The figure shows that the blue response increases with the plasma time and the red response decreases somewhat. The increase of the blue response is prone to errors since the value of the IQE for the reference cells is very low in this wavelength region, but seems nonetheless systematic. The increase is caused either by enhanced blue transmittance of the SiN_x:H layer, or improved surface passivation. Since we did not observe any significant changes in k, an improvement of the surface passivation is the most probable reason.

The observed changes in deposition rate and layer properties may be caused by the parasitic deposition on the quartz tubes. The refractive index n of the parasitic SiN_xH layer differs from that of quartz. This will change the net microwave power, and therefore the plasma conditions. We still cannot explain why this will result in better surface passivation and a higher deposition rate. With respect to the deposition rate we can mention that we observe an increase in deposition rate over even longer times of processing.

We conclude that the quality of the solar cells produced in the survey period of 20 h continuous processing improves slightly with time.

7. MODULE OUTDOOR STABILITY

Long-term stability of the performance of PV modules is a crucial issue for the PV industry. Warranty times of 20–25 years are quite usual for PV modules, and this requires not only that the encapsulation of the modules has

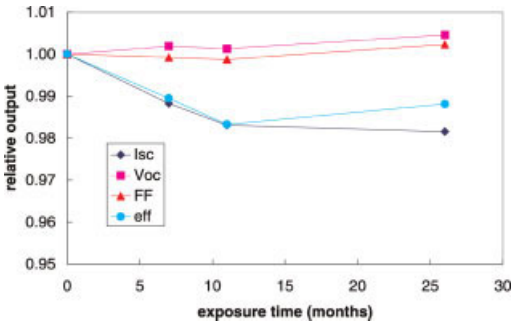

Figure 17. Two-year *I–V* monitoring results of module placed outdoors. Irradiance of the flash-tester was 1000 W/m^2

to be very well weather resistant (e.g., to prevent corrosion of electrical contacts, and delamination of EVA) but also that the electrical performance of the cells has to be stable on a long-term basis.[62] The key issue for the silicon nitride layers in this respect is the stability of the passivating properties under long-term irradiation. In particular the UV stability of the surface passivation has been a source of concern in the past.[7]

In order to monitor the long-term stability of cells with a SiN_x:H coating deposited by MW-PECVD, a module was manufactured at ECN in July 2000 in which 36 mc-Si cells were incorporated. The cells were made from 10×10 cm Baysix wafers, using a standard processing at ECN, as described in Section 5. The SiN_x:H coating was deposited using NH_3 and SiH_4 at conditions close to the optimum ones found in Section 6, using the system described in Section 2. The module was encapsulated with glass and EVA on the front side and Tedlar© at the rear side. After manufacturing, the module was placed on the roof of the ECN Solar Energy office building in Petten, and was regularly measured by an indoor flash-tester at ECN. The results of this monitoring are shown in Figure 17. It can be observed that the performance of the module was very stable over the entire monitoring period that lasted more than 2 years. A slight decrease of J_{sc} is found, but this decrease is partially compensated by a small increase of V_{oc}. The origin of the small increase of V_{oc} is unclear so far, but we may conclude that the cells—and therefore the SiN_x:H coatings—do not degrade during outdoor illumination. The power degradation over 2 years is less than 2% which is better than the 1-year average of 4·2% of 98 commercially available c-Si modules tested at LEEE-TISO.[63]

8. CONCLUSIONS

SiN_x:H coatings have become crucial components of commercial mc-Si solar cells. ECN and Roth&Rau Oberflächentechnik have jointly developed an industrial scale microwave PECVD system for deposition of such SiN_x:H layers. The layers have to fulfill three major requirements: (1) enhancement of the transmittance of light, by reduction of the reflection; (2) surface passivation; and (3) bulk passivation. The optimum SiN_x:H layer is a trade-off result of these three requirements, and therefore depends to some extent on other aspects of the cell. The emitter dopant concentration, e.g., determines the need and the effectiveness of surface passivation and the starting quality of the wafers determines the need and the effectiveness of bulk passivation.

We have shown that by using microwave PECVD, we are able to deposit SiN_x:H layers fulfilling all three requirements, both for N_2/SiH_4 and for NH_3/SiH_4 as process gases. Required optical properties can be obtained by tuning the N_2/SiH_4 or NH_3/SiH_4 gas flow ratio. For N_2/SiH_4 depositions, somewhat lower pressures have to be applied in order to achieve the same high total transmittance as for SiN_x:H layers deposited with NH_3/SiH_4. Best surface passivation is obtained for Si-rich layers, with a refractive index of 2·3 and higher, and this passivation is thermally stable for layers grown with N_2/SiH_4 and with NH_3/SiH_4. Effective recombination velocities on *p*-type FZ wafers coated with such layers are below 30 cm/s. Reasonably good surface passivation after thermal anneal (with S_{eff} on *p*-type FZ wafers in the range of 100 cm/s) can be obtained for layers with a refractive index of about 2·2. This latter result is of great practical relevance since the layers also have to provide bulk passivation by thermally enhanced hydrogenation of the wafers in the fabrication process of mc-Si wafers.

Good bulk passivation requires that the SiN_x:H layers are deposited at a certain minimum pressure. We have found a significant improvement of IQE between 900 and 1200 nm as a result of bulk passivation induced by firing of SiN_x:H layers. This improvement of the bulk lifetime of charge carriers leads to a gain of 20 mV and an increase of 10–15% of the total cell performance in comparison with cells on which a non-passivating TiO_2 layer was deposited as anti-reflection coating. Using an optimized SiN_x:H deposition process in a typically industrial inline fabrication process of mc-Si solar cells we have been able to produce cells with an efficiency of 16·5%.

We have shown that the deposition process, using microwave PECVD is a robust and stable process, in which optical properties and deposition rate varies less than 5% in a continuous processing period of 20 h.

For practical purposes, it is important that the SiN_x:H layers are stable on a long-term basis. Outdoor module stability experiments show that the passivating properties of SiN_x:H, deposited by microwave PECVD do not show any significant degradation after a time span of more than 2 years.

Acknowledgements

This work has been financed by the Netherlands Agency of Energy and Environment (NOVEM) in the projects ProDuSi and TOPR, and within the E.E.T. program by the Ministry of Economic Affairs, the Ministry of Education, Culture and Science and the Ministry of Public Housing, Physical Planning and Environment in the project Sunovation. The authors wish to thank Hermann Schlemm (Roth&Rau) for plasma density measurements and Junegie Hong (Eindhoven University of Technology) for measurements of optical properties of silicon nitride layers. Eric Kossen, Martien Koppes and Hans ter Beeke are thanked for technical assistance. Wim Sinke is acknowledged for the fruitful discussions on the presented work. Tom Moriarty and Keith Emery of NREL are acknowledged for performing *I–V* measurements.

REFERENCES

1. Doshi P, Jellison GE, Rohatgi A. Characterization and optimization of absorbing PECVD antireflection coatings for silicon photovoltaics. *Journal of Applied Optics* 1997; **36**: 7826.
2. Nagel H, Aberle AG, Hezel R. Optimised antireflection coatings for planar silicon solar cells using remote PECVD silicon nitride and porous silicon dioxide. *Progress in Photovoltaics: Research and Applications* 1999; **7**: 245–260.
3. Winderbaum S, Yun F, Reinhold O. Application of plasma enhanced chemical vapor deposition silicon nitride as a double layer antireflection coating and passivation layer for polysilicon solar cells. *Journal of Vacuum Science and Technology* 1997; **A15**: 1020–1025.
4. Hezel R, Schörner R. Plasma silicon nitride—a promising dielectric to achieve high-quality silicon MIS/IL solar cells. *Journal of Applied Physics* 1981; **52**: 3076.
5. Hezel R, Blumenstock K, Schörner R. Interface states and fixed charges in MNOS structures with APCVD and plasma silicon nitride. *Journal of the Electrochemical Society* 1984; **131**: 1679.
6. Leguijt C. *Surface Passivation for Silicon Solar Cells.* Thesis, Utrecht University, 1995.
7. Schuurmans F. *Surface Passivation of Silicon by PECVD Silicon Nitride.* Thesis, Utrecht University, 1998.
8. Schmidt J. *Untersuchungen zur Ladungsträgerrekombination and den Oberflächen und im Volumen von kristallinen Silicium-Solarzellen.* Thesis, Hannover University, 1998.
9. Aberle AG, Hezel R. Progress in low-temperature surface passivation of silicon solar cells using remote-plasma silicon nitride. *Progress in Photovoltaics: Research and Applications* 1997; **5**: 29–50.
10. Aberle AG. *Crystalline Silicon Solar Cells: Advanced Surface Passivation and Analysis.* The University of New South Wales, 1999.
11. Schmidt J, Aberle AG. Carrier recombination at silicon–silicon nitride interfaces fabricated by plasma-enhanced chemical vapor deposition. *Journal of Applied Physics* 1999; **85**: 3626–3633.
12. Schmidt J, Kerr M. Highest-quality surface passivation of low-resistivity *p*-type silicon using stoichiometric PECVD silicon nitride. *Solar Energy Materials and Solar Cells* 2001; **65**: 585–591.
13. Lenkeit B, Hezel R. Improved understanding of the surface-passivating properties of RPECVD silicon nitride on *p*-type crystalline silicon. *Proceedings of the 17th European Photovoltaic Solar Energy Conference*, Munich, Germany, 22–26 October 2001; 343–346.

14. Lenkeit B, Steckemetz S, Artuso F, Hezel R. Excellent thermal stability of remote plasma-enhanced chemical vapour deposited silicon nitride films for the rear of screen-printed bifacial silicon solar cells. *Solar Energy Materials and Solar Cells* 2001; **65**: 317–323.
15. Mäckel H, Lüdemann R. Detailed study of the composition of hydrogenated SiN_x layers for high-quality silicon surface passivation. *Journal of Applied Physics* 2002; **92**: 2602–2609.
16. Cuevas A, Kerr M, Schmidt J. Passivation of crystalline silicon using silicon nitride. *Proceedings of the 3rd World Conference on Photovoltaic Energy Conversion*, Osaka, Japan, 11–18 May 2003; 913–918.
17. Kimura K. Recent developments in polycrystalline silicon solar cells. *Technical Digest, International PVSEC-1*, Kobe, November 1984; 3741.
18. Schmidt J, Kerr M, Cuevas A. Surface passivation of silicon solar cells using plasma-enhanced chemical-vapour-deposited SiN films and thin thermal SiO_2/plasma SiN stacks. *Semiconductor Science and Technology* 2001; **16**: 164–170.
19. Mittelstädt L, Dauwe S, Metz A, Hezel R, Hässler C. Front and rear silicon-nitride-passivated multicrystalline silicon solar cells with an efficiency of 18·1%. *Progress in Photovoltaics: Research and Applications* 2002; **10**: 35–39.
20. Chen Z, Rohatgi A, Bell RO, Kalejs JP. Defect passivation in multicrystalline-Si materials by plasma-enhanced chemical vapor deposition of SiO_2/SiN coatings. *Applied Physics Letters* 1994; **65**: 2078–2080.
21. Duerinckx F. *Bulk and surface passivation of screen printed multicrystalline silicon solar cells based on plasma enhanced CVD of silicon nitride.* Thesis, Leuven University, 1999.
22. Einhaus R, Duerinckx F, Van Kerschaver E, Szlufcik J, Durand F, Riberyron PJ, Duby JC, Sarti D, Goaer G, Le GN, Périchaud I, Clerc L, Martinuzzi S. Hydrogen passivation of newly developed EMC-multi-crystalline silicon. *Materials Science and Engineering* 1999; **B58**: 81–85.
23. Jeong JW, Rosenblum MD, Kalejs JP, Rohatgi A. Hydrogenation of defects in edge-defined film-fed grown aluminum-enhanced plasma enhanced chemical vapor deposited silicon nitride multicrystalline silicon. *Journal of Applied Physics* 2000; **87**: 7551–7557.
24. Soppe W, Weeber A, de Moor H, Sinke W, Lauinger T, Auer R, Lenkeit B, Aberle A. Cost effective mc-Si processing by screenprinting on remote PECVD layers. *Proceedings of the 2nd World Conference and Exhibition on Photovoltaic Solar Energy Conversion*, Vienna, Austria, 6–10 July 1998; 1826–1828.
25. Soppe WJ, Devilee C, Schiermeier SEA, Hong J, Kessels WMM, Van de Sanden MCM, Arnoldbik WM, Weeber AW. Bulk and surface passivation by silicon nitride grown by remote microwave PECVD. *Proceedings of the 17th European Photovoltaic Solar Energy Conference*, Munich, Germany, 22–26 October 2001; 1543–1546.
26. Duerinckx F, Szlufcik J. Defect passivation of industrial multicrystalline solar cells based on PECVD silicon nitride. *Solar Energy Materials and Solar Cells* 2002; **72**: 231–246.
27. Geerligs LJ, Azzizi A, Macdonald DH, Manshanden P. Hydrogen passivation of iron in multicrystalline silicon. *Proceedings of the 13th Workshop on Crystalline Silicon Solar Cell Materials and Processes*, Colorado, USA, 10–13 August 2003; 199–202.
28. Pankove JI, Johnson NM. *Hydrogen in Semiconductors.* Academic Press: New York, 1991.
29. Sopori BL, Deng X, Benner JP, Rohatgi A, Sana P, Estreicher SK, Park YK, Roberson MA. Hydrogen in silicon: a discussion of diffusion and passivation mechanisms. *Solar Energy Materials and Solar Cells* 1996; **41/42**: 159–169.
30. Nickel NH, Kaiser I. Hydrogen migration in phosphorous doped polycrystalline silicon. *Materials Research Society Symposium Proceedings* 1998; **513**: 165–170.
31. Boehme C, Lucovsky G. H loss mechanism during anneal of silicon nitride: chemical dissociation. *Journal of Applied Physics* 2000; **88**: 6055–6059.
32. Sopori B, Zhang Y, Ravindra NM. Silicon device processing in H-ambients: H-diffusion mechanisms and influence on electronic properties. *Journal of Electronic Materials* 2001; **30**: 1616–1627.
33. Rohatgi A, Yelundur V, Jeong J, Ebong A, Rosenblum MD, Hanoka JI. Fundamental understanding and implementation of Al-enhanced PECVD SiN_x hydrogenation in silicon ribbons. *Solar Energy Materials and Solar Cells* 2002; **74**: 117–126.
34. Hong J, Kessels WMM, Soppe WJ, Weeber AW, Arnoldbik WM, Van de Sanden MCM. Influence of the high-temperature 'firing' step on high-rate plasma deposited silicon nitride films used as bulk passivating antireflection coatings on silicon solar cells. *Journal of Vacuum Science Technology B* 2003; **21**: 2123–2132.
35. Job R, Fahrner WR, Kazuchits NM, Ulyashin AG. A two-step low-temperature process for a *p–n* junction formation due to hydrogen enhanced thermal donor formation in *p*-type Czochralski silicon. *Materials Research Society Symposium Proceedings* 1998; **513**: 337–342.
36. Rashkeev SN, Di Ventra M, Pantelides ST. Hydrogen passivation and activation of oxygen complexes in silicon. *Applied Physics Letters* 2001; **78**: 1571–1573.
37. Aberle AG, Lauinger T, Hezel R. Remote PECVD silicon nitride—a key technology for the crystalline silicon PV industry of the 21st century? *Proceedings of the 14th European Photovoltaic Solar Energy Conference*, Barcelona, Spain, 30 June–4 July 1997; 684–689.

38. Soppe WJ, Duijvelaar BG, Schiermeier SEA, Weeber AW, Steiner A, Schuurmans FM. A high-throughput PECVD reactor for deposition of passivating SiN layers. *Proceedings of the 16th European Photovoltaic Solar Energy Conference*, Glasgow, UK, 1–5 May 2000; 1420–1423.
39. Schitthelm F, Völk P, Dekkers H, Szlufcik J. Quasi continuous a-SiN:H-PECVD system with high throughput rate for solar cell AR-coating. *Proceedings of the 16th European Photovoltaic Solar Energy Conference*, Glasgow, UK, 1–5 May 2000; 1609–1612.
40. Coates K, Morrison S, Narayanan S, Madan A. Deposition of silicon nitride to improve the conversion efficiency of multicrystalline silicon solar cells. *Proceedings of the 16th European Photovoltaic Solar Energy Conference*, Glasgow, UK, 1–5 May 2000; 1279–1281.
41. http://www.otb.nl/Media/Leaflet_DEPx_met_foto.pdf
42. Von Aichberger S. Deeper than blue. Market survey on deposition systems for silicon nitride. *Photon International* 2003; **3**: 50–55.
43. Culik JS, Faller F, Goncharovsky IS, Rand JA, Barnett AM. Progress on 15 MW single thread silicon-film^{TM} solar cell manufacturing systems. *Proceedings of the 17th European Photovoltaic Solar Energy Conference*, Munich, Germany, 22–26 October 2001; 1347–1350.
44. Nybergh K. Using factorial design and response surface methodology to optimize growth parameters of PECVD grown silicon nitride. *Physica Scripta* 1999; **T79**: 266–271.
45. Moisan M, Pelletier J. *Microwave Exited Plasmas.* Elsevier: Amsterdam, 1992; 123–180.
46. Lieberman MA, Lichtenberg AJ. *Principles of Plasma Discharges and Materials Processing.* Wiley: New York, 1994.
47. Petasch W, Räuchle E, Muegge H, Muegge K. Duo plasmaline—a linearly extended homogeneous low pressure plasma source. *Surface and Coatings Technology* 1997; **93**: 112–118.
48. Räuchle E. Duo-plasmaline, a surface wave sustained linearly extended discharge. *Journal de Physique IV France* 1998; **8**(Pr7): 99–107.
49. Lauinger T, Moschner J, Aberle AG, Hezel R. Optimization and characterization of remote plasma-enhanced chemical vapor deposition silicon nitride for the passivation of *p*-type crystalline surfaces. *Journal of Vacuum Science and Technology A* 1998; **16**: 530–543.
50. Smith DL. Plasma deposition of SiN_xH_y: process chemistry vs film properties. *Materials Research Society Symposium Proceedings* 1990; **165**: 69–77.
51. Hanyaloglu BF, Aydil ES. Low temperature plasma deposition of silicon nitride from silane and nitrogen plasmas. *Journal of Vacuum Science and Technology* 1998; **A16**: 2794–2803.
52. Kessels WMM, van Assche FJH, Hong J, Schramm DC, van de Sanden MCM. Plasma diagnostic study of silicon nitride film growth in a remote Ar-H_2-N_2-SiH_4 plasma: role of N and SiH_n radicals. *Journal of Vacuum Science and Technology A* 2004; **22**: 96–106.
53. Robertson J. Electronic structure of silicon nitride. *Philosophical Magazine B* 1991; **63**: 47–77.
54. Giorgis F, Giuliani F, Pirri CF, Tesso E. Optical, structural and electrical properties of device quality hydrogenated amorphous silicon-nitrogen films deposited by plasma-enhanced chemical vapour deposition. *Philosophical Magazine B* 1998; **77**: 925–944.
55. Rieffe HC, Soppe WJ, Kessels WMM, Van de Sanden MCM, Weeber AW. Passivation on mc-Si solar cells with PECVD SiN_x:H using N_2 and SiH_4. *Proceedings of PV in Europe from PV Technology to Energy Solutions*, Rome, Italy, 7–11 October 2002; 295–298.
56. Sinton RA, Cuevas A. Contactless determination of current—voltage characteristics and minority-carrier lifetimes in semiconductors from quasi-steady-state photoconductance data. *Applied Physics Letters* 1996; **69**: 2510–2512.
57. Moschner JD, Henze J, Schmidt J, Hezel R. High-quality surface passivation of silicon solar cells in an industrial-type inline plasma silicon nitride deposition system. *Progress in Photovoltaics: Research and Applications* 2004; **12**: 21–31.
58. Shanks HR, Lye L. Formation of pin holes in hydrogenated amorphous silicon at high temperatures and the yield strength of a-Si:H. *Journal of Applied Physics* 1981; **52**: 811–813.
59. Hauser A, Spiegel M, Fath P, Bucher E. Influence of an ammonia activation prior to the PECVD SiN deposition on the solar cell performance. *Solar Energy Materials and Solar Cells* 2003; **75**: 357–362.
60. http://www.statgraphics.com
61. Weeber AW, Sinke WC. Statistical analysis for solar cell research. *Proceedings of the 25th IEEE*, Washington DC, 1996; 565.
62. IEC 61215. *Crystalline silicon terrestrial photovoltaic (PV) modules—Design qualification and type approval* 1993.
63. Chianese D, Realini A, Cereghetti N, Rezzonico S, Bura E, Friesen G, Bernasconi A. Analysis of weathered c-Si PV modules. *Proceedings of the 3rd World Conference on Photovoltaic Energy Conversion*, Osaka, Japan, 11–18 May 2003; 2922–2926.

